

Seeing Differently, Acting Similarly: Imitation Learning with Heterogeneous Observations

Xin-Qiang Cai¹, Yao-Xiang Ding¹, Zi-Xuan Chen¹, Yuan Jiang¹, Masashi Sugiyama^{2,3}, Zhi-Hua Zhou¹

¹National Key Laboratory for Novel Software Technology Nanjing University, Nanjing, China.

²RIKEN Center for Advanced Intelligence Project, Tokyo, Japan.

³The University of Tokyo, Tokyo, Japan.

Abstract

In many real-world imitation learning tasks, the demonstrator and the learner have to act in different but full observation spaces. This situation generates significant obstacles for existing imitation learning approaches to work, even when they are combined with traditional space adaptation techniques. The main challenge lies in bridging expert’s occupancy measures to learner’s dynamically changing occupancy measures under the different observation spaces. In this work, we model the above learning problem as *Heterogeneous Observations Imitation Learning* (HOIL). We propose the *Importance Weighting with REjection* (IWRE) algorithm based on the techniques of importance-weighting, learning with rejection, and active querying to solve the key challenge of occupancy measure matching. Experimental results show that IWRE can successfully solve HOIL tasks, including the challenging task of transforming the vision-based demonstrations to random access memory (RAM)-based policies under the Atari domain.

1. Introduction

In real-world imitation learning (IL) problems, the expert and the learner usually have their own observations of the same states from the environment. For example, in Figure 1, an autonomous agent is learning to drive by imitating a human expert. The expert takes her actions mainly based on auditory and visual observations, which are familiar to human beings. However, the learning agent does not necessarily use the same way to observe: it can utilize more machine-capable sensors such as a LiDAR, radar, and bird-eye view (BEV) map to generate its observations [19]. The key feature behind this example is that: Both the expert and the learner have their different *full observations* of the *same state* of the environment, thus they essentially have to choose the same action if acting optimally. We call this problem Heterogeneous Observations IL (HOIL). Existing IL algorithms are invalid for the HOIL problem since they usually assume the agreement of expert’s and learner’s observation spaces.

Even though HOIL is novel for IL, some similar scenarios have been studied in supervised learning. Multi-view learning [20, 31] assumes that data from multiple views are available during learning. In domain adaptation [4, 11], the target domain could have a significantly different distribution to the source domain. In feature evolvable stream learning [14, 15, 33], the input space could change in different learning stages. Can we trivially combine the existing IL approaches with techniques from these supervised learning scenarios directly to solve the HOIL problem? The answer is unfortunately no. In HOIL, the learner not only needs to deal with the difference between observation spaces, but also needs to deal with the dynamical

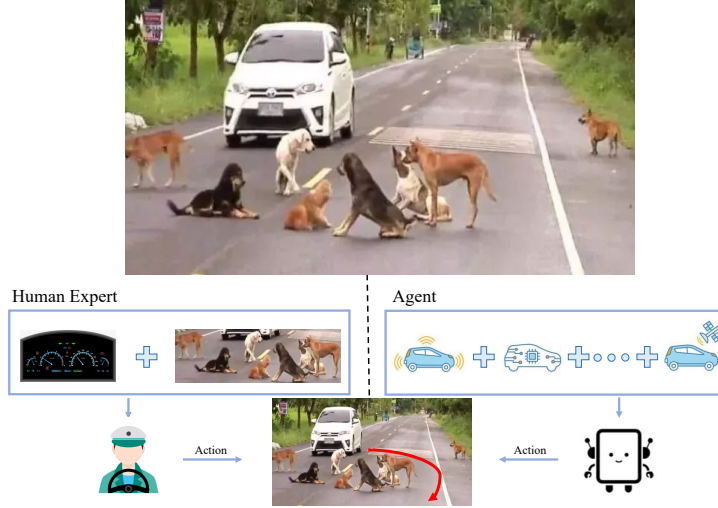


Figure 1: Autonomous driving: an example of the HOIL problem. Both Figures 1 and 2 include some illustrations and pictures from the Internet (source: www.vecteezy.com).

change of the learner’s occupancy measure resulted from the frequent improvement of the policy. This issue cannot be solved by supervised learning techniques, which are usually designed for dealing with the fixed differences between two static distributions. This also makes some IL approaches aiming at addressing the static domain changes during learning incapable for HOIL [26, 18].

In this paper, we initialize the study of the HOIL problem. We propose a three-stage process for solving the HOIL problem. To tackle both the difference between observation spaces and the dynamical change of the occupancy measure, we resort to the techniques of *importance-weighting* [28, 10] and *learning with rejection* [7, 12] as well as *active querying* to propose the Importance Weighting with REjection (IWRE) approach. We evaluate the efficacy of IWRE with benchmark tasks in MuJoCo [29], as well as the challenging task of imitating vision-based experts for RAM-based learners in Atari [3]. The results show that IWRE can outperform existing IL algorithms significantly for HOIL tasks.

2. Related Work

Domain-Shifted IL. There exist many remarkable studies about Domain-Shifted IL (DSIL), aiming at addressing the *static distributional shift* of the optimal policies resulted from the environmental differences *under the same observation space*. [26, 25, 22] studied the situation where the demonstrations are in view of the third person. [18, 17] addressed the imitation learning problem in which the domain shift appears between the distributions of the demonstrations and the agent’s environment. [16] learned an agent in the simulator through demonstrations in the real environment. [26, 28, 8] focused on the calibration for the mismatch between simulators and the real world through some transfer learning styles. There are two major differences of HOIL to DSIL: One is that HOIL considers heterogeneous observation spaces instead of a homogeneous one; another is that in HOIL, instead of only considering the difference between two fixed policies, dealing with the dynamic change of the learner’s policy during learning is essential. Thus HOIL is a relatively more challenging problem than DSIL.

POMDP. The problem of partially observable Markov decision processes (POMDPs), in which only partial observation instead of the original observation can be received by the agent(s), has been studied in the context of multi-agent problems [32, 23, 2]. But distinct from HOIL, in a POMDP, the agents only have *partial* observations of the true states, which would become an obstacle for them to make decisions correctly. While in HOIL, both the expert’s and the learner’s observations are *full* in the sense that the observations themselves are not the obstacle for acting perfectly. Instead, the main challenge for HOIL is to deal with the mismatches between the observation spaces, in order to make the learner successfully imitate the expert’s policy.

3. The HOIL Problem

In this section, we first introduce some preliminaries and then formulate the HOIL problem.

3.1. Preliminaries

A HOIL problem is defined within a Markov decision process with multiple observation spaces, i.e. $\langle \mathcal{S}, \{\mathcal{O}\}, \mathcal{A}, \mathcal{P}, \gamma \rangle$, where \mathcal{S} denotes the state space, $\{\mathcal{O}\}$ denotes a set of observation spaces, \mathcal{A} denotes the action space, $\mathcal{P} : \mathcal{S} \times \mathcal{A} \times \mathcal{S} \rightarrow \mathbb{R}$ denotes the transition probability distribution of the state and action and $\gamma \in (0, 1]$ denotes the discount factor. Furthermore, a policy π over an observation space \mathcal{O} is defined as a function mapping from \mathcal{O} to \mathcal{A} , and we denote by $\Pi_{\mathcal{O}}$ the set of all policies over \mathcal{O} . In HOIL, both the expert and the learner have their own observation spaces, which are denoted as \mathcal{O}_E and \mathcal{O}_L respectively. Both \mathcal{O}_E and \mathcal{O}_L are assumed to be *full observation spaces* such that there exist two *bijective mappings* $f_E : \mathcal{S} \rightarrow \mathcal{O}_E, f_L : \mathcal{S} \rightarrow \mathcal{O}_L$, which are unknown functions mapping the underlying true states to the observations. It is obvious to see that by this assumption, any policy over \mathcal{O}_E has a unique correspondence over \mathcal{O}_L . This makes HOIL possible since the target of HOIL is to find the corresponding policy of the expert policy under \mathcal{O}_L .

Denote by x an observation-action pair (o, a) , which is called an instance. Furthermore, define the *occupancy measure* of a policy π under an observation space \mathcal{O} as $\rho_{\pi} : \mathcal{O} \times \mathcal{A} \rightarrow \mathbb{R}$ such that $\rho_{\pi}(o, a) = \pi(a|o) \sum_{t=0}^{\infty} \gamma^t \Pr(o_t = o | \pi)$. Under HOIL, the learner accesses the expert demonstrations $\tilde{\mathcal{T}}_{\pi_E}$, which is a set of instances sampled from ρ_{π_E} . As discussed previously, the goal of HOIL is to learn a policy $\hat{\pi}$ as the corresponding policy of π_E over \mathcal{O}_L . If $\mathcal{O}_E = \mathcal{O}_L$, HOIL degenerates to traditional IL. GAIL [13] is one of the state-of-the-art IL approaches under this situation, which tries to minimize the divergence between the learner and expert occupancy measures $d(\rho_{\hat{\pi}}, \rho_{\pi_E})$. The objective of GAIL is

$$\min_{\hat{\pi}} \max_D \mathbb{E}_{x \sim \rho_{\pi_E}} [\log D(x)] + \mathbb{E}_{x \sim \rho_{\hat{\pi}}} [\log(1 - D(x))] - \mathbb{H}(\hat{\pi}), \quad (1)$$

where $\mathbb{H}(\hat{\pi})$ is the causal entropy performed as a regularization term, and $D : \mathcal{O}_E \times \mathcal{A} \rightarrow [0, 1]$ is the discriminator between π_E and $\hat{\pi}$. GAIL solves (1) by alternatively taking a gradient ascent step to train the discriminator D , and a minimization step to learn policy $\hat{\pi}$ based on an off-the-shelf reinforcement learning (RL) algorithm with the pseudo reward $-\log D(x)$.

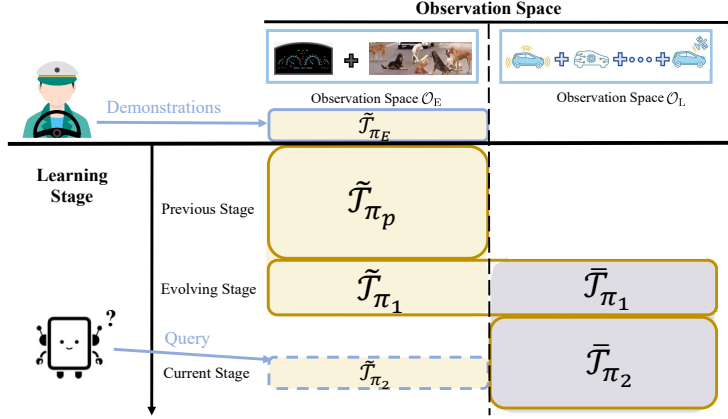


Figure 2: Illustration for the three-stage process for solving HOIL.

3.2. The Three-Stage Process for Solving HOIL

Now we are ready to introduce a three-stage process for solving HOIL, which we argue that any algorithms for HOIL should follow. The key idea lies in obtaining an initial policy over \mathcal{O}_E at the first stage, under which the learner accesses \mathcal{O}_E only. The initial policy needs not be optimal under \mathcal{O}_E . Thus if \mathcal{O}_E is expensive for the learner to act in reality, the first stage can be carried out within *economic but inaccurate environments*, such as simulators. Afterward, at the following two stages, the initial policy is transformed to \mathcal{O}_L by building the connection between \mathcal{O}_E and \mathcal{O}_L , *under the real environment*, in which \mathcal{O}_L is always available to the learner. Building this connection is the biggest challenge for HOIL, and we argue that this could not be achieved by allowing *observation coexistence* (OC): At some steps of learning, besides the observations from \mathcal{O}_L , the learner could also request the corresponding observations from \mathcal{O}_E . On the other hand, since the learner uses only \mathcal{O}_L to make her decisions, the more times OC is requested, the more waste on requesting \mathcal{O}_E . This reminds us to minimize the number of times to request OC. An overview of this learning process is shown in Figure 2.

Previous stage. The previous stage is carried out within \mathcal{O}_E . With the expert demonstrations $\tilde{\mathcal{T}}_{\pi_E}$, the learner is assumed to utilize GAIL to obtain an initial policy π_1 as well as a discriminator D_1 , both over \mathcal{O}_E . An initial dataset $\tilde{\mathcal{T}}_{\pi_p}$ is also collected by sampling from ρ_{π_1} . As described above, the previous stage can be carried out within an economic environment where accessing \mathcal{O}_E is inexpensive.

Evolving stage. At the evolving stage, both \mathcal{O}_E and \mathcal{O}_L are always available, thus OC is always requested. the learned policy π_1 is executed to generate samples \mathcal{T}_{π_1} by sampling from ρ_{π_1} , in which each instance contains both two observations. To minimize the number of times that OC is requested, we assume that the number of samples is much fewer than those in the previous and next stages. We denote \mathcal{T}_{π_1} in \mathcal{O}_E space as $\tilde{\mathcal{T}}_{\pi_1}$, and that in \mathcal{O}_L space as $\bar{\mathcal{T}}_{\pi_1}$.

Current stage. The current stage is carried out within \mathcal{O}_L . The target is to learn a policy π_2 over \mathcal{O}_L , which is the final policy to learn. We denote by $\bar{\mathcal{T}}_{\pi_2}$ the dataset generated from ρ_{π_2} . Furthermore, at this stage, an *active query strategy* is allowed to request OC for a small subset of instances from $\bar{\mathcal{T}}_{\pi_2}$, in order to collect a small dataset $\tilde{\mathcal{T}}_{\pi_2}$ over \mathcal{O}_E .

4. Imitation Learning with Importance-Weighting and Rejection

For the HOIL problems, the most difficult part lies in the learning procedure of π_2 . So in this section, we focus on the challenges of learning a good π_2 and propose a novel algorithm named *Importance Weighting with REjection* (IWRE) to solve these challenges.

4.1. Dynamics Mismatch and Importance-Weighting

To analyze the learning process, we let ρ_{π_E} be the occupancy distribution of the expert demonstrations, ρ_{π_1} be that of the data in the evolving stage, and ρ_{π_2} be that of the data in the current stage. Since π_1 is imperfect, we can regard the distribution of the evolving data ρ_{π_1} as the mixture of ρ_{π_E} and $\rho_{\pi_{NE}}$, depicted in Figure 3(a), in which $\rho_{\pi_{NE}}$ is the distribution of the non-expert data. In the current stage, the original objective of π_2 is to imitate the latent policy of the expert through demonstrations. To this end, the original objective of reward function D_{w_2} for π_2 is to optimize

$$\max_{w_2} \mathbb{E}_{x \sim \rho_{\pi_2}} \log D_{w_2}(x) + \mathbb{E}_{x \sim \rho_{\pi_E}} \log[1 - D_{w_2}(x)]. \quad (2)$$

But since the expert demonstrations are only available in the \mathcal{O}_E space, in the current stage, we can only utilize the data in the evolving stage $\bar{x}_{\pi_1} \sim \rho_{\pi_1}$ to learn π_2 and D_{w_2} . Besides, as π_1 is an imperfect policy, directly imitating \bar{x}_{π_1} could reduce the performance of the optimal π_2 to that of π_1 . So we use the importance-weighting technique to calibrate this dynamics mismatch, i.e.,

$$\max \mathcal{L}(D_{w_2}) \triangleq \mathbb{E}_{x \sim \rho_{\pi_2}} \log D_{w_2}(x) + \mathbb{E}_{x \sim \rho_{\pi_1}} \alpha(x) \log[1 - D_{w_2}(x)], \quad (3)$$

where $\alpha(x) \triangleq \frac{\rho_{\pi_E}}{\rho_{\pi_1}}$ is the importance-weighting factor [10]. So the current issue lies in how to estimate $\frac{\rho_{\pi_E}}{\rho_{\pi_1}}$. To achieve this purpose, we need to bridge expert demonstrations and evolving data. On the other hand, we have had a reward function D_{w_1} in view of the \mathcal{O}_E space with sufficient training, and its optimizing target is

$$\max \mathcal{L}(D_{w_1}) \triangleq \mathbb{E}_{x \sim \rho_{\pi_1}} \log D_{w_1}(x) + \mathbb{E}_{x \sim \rho_{\pi_E}} \log[1 - D_{w_1}(x)]. \quad (4)$$

If we write the training criterion (4) in form of integral, i.e.,

$$\max \mathcal{L}(D_{w_1}) = \int_x \rho_{\pi_1} \log D_{w_1} + \rho_{\pi_E} \log[1 - D_{w_1}] dx, \quad (5)$$

then, by setting the derivative of the objective (5) to 0 ($\frac{\partial \mathcal{L}}{\partial D_{w_1}} = 0$), we can obtain the optimum D_{w_1} :

$$D_{w_1}^* = \frac{\rho_{\pi_1}}{\rho_{\pi_1} + \rho_{\pi_E}}, \quad (6)$$

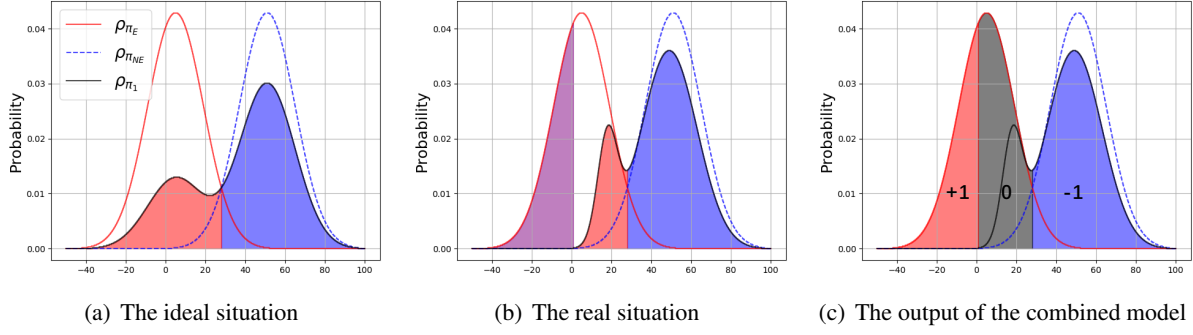


Figure 3: The comparisons among the distributions of expert demonstrations, evolving data, and non-expert data. ρ_{π_1} can be regarded as a mixture of ρ_{π_E} and $\rho_{\pi_{NE}}$, in which the red and blue regions denote the expert and non-expert parts of ρ_{π_1} respectively. (a) The ideal distribution, where $\text{supp}(\rho_{\pi_E})$ is totally covered by $\text{supp}(\rho_{\pi_1})$; (b) The real-world situation, where there exists part of $\text{supp}(\rho_{\pi_E})$ that $\text{supp}(\rho_{\pi_1})$ does not cover. The purple region in ρ_{π_E} denotes the invisible part (the uncovered $\text{supp}(\rho_{\pi_E})$) for ρ_{π_1} . (c) The output of the combined model $\langle \mathbb{I}[D_{w_1}], g_1 \rangle$, where $\mathbb{I}[\cdot]$ takes +1 if $\cdot > 0.5$, and -1 otherwise. The red (+1), black (0), and blue (−1) regions denote the latent demonstrations, the observed demonstrations, and the non-expert data respectively.

in which the Leibniz rule was used to exchange the order of differentiation and integration. Besides, in the evolving stage, we can train D_{w_1} using the evolving data $\tilde{\mathcal{T}}_{\pi_1}$ and the expert demonstrations $\tilde{\mathcal{T}}_{\pi_E}$. Then D_{w_1} is sufficient to estimate the importance-weighting factor, i.e.,

$$\alpha(x) \triangleq \frac{\rho_{\pi_E}}{\rho_{\pi_1}} = \frac{1 - D_{w_1}^*}{D_{w_1}^*} \approx \frac{1 - D_{w_1}}{D_{w_1}}. \quad (7)$$

In this way, we can use D_{w_1} , which contains the information in the previous stage, to calibrate the learning process of D_{w_2} , and thereby improve the performance of π_2 . The final optimization objective for D_{w_2} is

$$\max \mathcal{L}(D_{w_2}) = \mathbb{E}_{x \sim \rho_{\pi_2}} \log D_{w_2}(x) + \mathbb{E}_{x \sim \rho_{\pi_1}} \frac{1 - D_{w_1}}{D_{w_1}} \log[1 - D_{w_2}(x)]. \quad (8)$$

In this way, D_{w_2} can effectively dig out the expert part of ρ_{π_1} and produce efficient rewards for π_2 .

4.2. Support Mismatch

The importance-weighting is utilized to make D_{w_2} learn from the expert part of the evolving data more and the non-expert part less. The prerequisite for the HOIL problem to be completely solved lies that the support set of ρ_{π_1} could cover the support set of ρ_{π_E} (the support set is defined in Definition 1), i.e., $\text{supp}(\rho_{\pi_E}) \subseteq \text{supp}(\rho_{\pi_1})$, to make sure the expectation under ρ_{π_1} can be fitted into the expectation under ρ_{π_E} . However, in real situations, there may exist some parts of the support set of ρ_{π_E} that ρ_{π_1} does not cover (i.e., $\text{supp}(\rho_{\pi_E}) \not\subseteq \text{supp}(\rho_{\pi_1})$, see Figure 3(b)). Because the imperfection of π_1 comes from not only the non-expert part but also the unexplored area of ρ_{π_E} [30].

Definition 1 (Support Set). *The support set of a real-valued function ρ is the subset of the domain containing the elements which are not mapped to zero:*

$$\text{supp}(\rho) = \{x \in \mathcal{T} | \rho(x) \neq 0\}. \quad (9)$$

Besides, we can observe that the optimization term of D_{w_2} in Equation (8) is based on ρ_{π_1} , while $\text{supp}(\rho_{\pi_E}) \not\subseteq \text{supp}(\rho_{\pi_1})$, which means that there exist some unseen parts (the purple region in Figure 3(b)) of ρ_{π_E} that D_{w_2} cannot access. We refer to these unseen parts as the latent demonstrations, and the expert part of ρ_{π_1} (the red region) as the observed demonstrations. In this case, D_{w_2} cannot reward π_2 effectively, even if π_2 has generated samples similar to the latent demonstrations.

4.3. Imitation Learning with Rejection

Based on the above discussion, what we need to do is to find out the representations of the latent demonstrations in the \mathcal{O}_L space. Meanwhile, due to the constant change in distributions, we need to dynamically bridge the \mathcal{O}_E and \mathcal{O}_L spaces to dig out this representation through several queries on the \mathcal{O}_E observation of the current data $\bar{\mathcal{T}}_{\pi_2}$.

However, we cannot directly map the latent demonstrations $\mathcal{O}_E \rightarrow \mathcal{O}_L$, because we cannot access ρ_{π_E} in the \mathcal{O}_L space. On the other hand, since we have the evolving data $\{\tilde{\mathcal{T}}_{\pi_1}, \bar{\mathcal{T}}_{\pi_1}\} \sim \rho_{\pi_1}$ in the \mathcal{O}_E and \mathcal{O}_L spaces respectively, we can learn a hyperplane in the \mathcal{O}_E space, which should be able to cover ρ_{π_E} meanwhile differentiate the latent and observed demonstrations. Next we can deliver this hyperplane into the \mathcal{O}_L space through $\{\tilde{\mathcal{T}}_{\pi_1}, \bar{\mathcal{T}}_{\pi_1}\}$. Afterward, we can utilize the delivered hyperplane to judge whether the instance in the \mathcal{O}_L space is the instance of the latent demonstrations. Moreover, we can query the \mathcal{O}_E observation of the instance to check the judgment, and further update the delivered hyperplane.

In this work, we learn a rejection model to represent the hyperplane mentioned above, i.e., $g_1 : \mathcal{O}_E \times \mathcal{A} \rightarrow \{0, 1\}$, which could differentiate these three regions (the purple, red, and blue regions in Figure 3(b)) in the \mathcal{O}_E space by combining g_1 with D_{w_1} . In the \mathcal{O}_L space, we align g_1 into $g_2 : \mathcal{O}_L \times \mathcal{A} \rightarrow \{0, 1\}$, which is used to check whether \bar{x}_{π_2} belongs to the latent demonstrations. The rejection setting is the same as that in [7], and inspired by [12], the optimization objective of the combination of the reward function D_w and the rejection model g is

$$\mathcal{L}(D_w, g) \triangleq \hat{l}(D_w, g) + \lambda \max(0, c - \hat{\phi}(g))^2, \quad (10)$$

where c denotes the target coverage, and λ denotes the factor for controlling the relative importance of rejection. Besides, the empirical coverage $\hat{\phi}(g)$ is defined as

$$\hat{\phi}(g|X) \triangleq \frac{1}{m} \sum_{i=1}^m g(x_i), \quad (11)$$

and the empirical rejection risk $\hat{l}(D_w, g)$ is defined as

$$\hat{l}(D_w, g) \triangleq \frac{\frac{1}{m} \sum_{i=1}^m \mathcal{L}(D_w(x_i)) \cdot g(x_i)}{\hat{\phi}(g)}. \quad (12)$$

4.4. IWRE

Here we combine the importance-weighting and rejection into a unified whole, to propose a novel algorithm named IWRE (Importance Weighting with REjection). Concretely, in the previous stage, we train the policy π_1 and reward function D_{w_1} in the \mathcal{O}_E space using GAIL [13] in low-dimensional environments or HashReward [6] in high-dimensional environments; in the evolving stage, we convert the binary classifier

D_{w_1} into the rejection model g_1 (see Figure 3(c)), and then align g_1 into g_2 using the evolving data; for the given current data $\bar{x}_i \in \mathcal{O}_L \times \mathcal{A}$, if the output of $g_2(\bar{x}_i) = 1$, which means g_2 regards this data as being belonging to the latent demonstrations, then we query the \mathcal{O}_E observation of this data (denoted as $\tilde{x}_i \in \mathcal{O}_E \times \mathcal{A}$), and input it into g_1 (if $g_1(\tilde{x}_i) = 1$, then this data could belong to the latent demonstrations *w.h.p.*). Next we use the data and the output of g_1 to update D_{w_2} and g_2 . The learning procedure of our algorithm is provided in the appendix.

5. Experiment

In this section, we validate our algorithm on Atari 2600 [3] (GPL License) and MuJoCo [29] (Academic License) domains. The experiments are designed to investigate the following questions:

- 1) Can IWRE achieve significant performance under HOIL tasks?
- 2) Can IWRE deal with the support mismatch problem?
- 3) At the current stage, whether active querying for HOIL is indeed necessary?

Below we first introduce the experimental setup and then investigate the above questions. More results and experimental details are included in the appendix.

5.1. Experimental Setup

Environments. We choose 3 games in Atari and 5 simulators in MuJoCo. The experiments are conducted in OpenAI Gym platform [5] (MIT License), which contains Atari 2600 video games with visual (raw-pixel) or 128-byte random access memory (RAM) observation space, as well as MuJoCo control tasks with signal-based observation spaces. To generate \mathcal{O}_E and \mathcal{O}_L in HOIL, for MuJoCo, we randomly divide the original observation spaces into two parts. For Atari, we set the visual space as \mathcal{O}_E and the RAM space as \mathcal{O}_L . We train converged DQN-based agents as experts in Atari, and DDPG-based [21] agents in MuJoCo. 20 expert trajectories are collected for each game. 5 trials with different random seeds are conducted for each environment. All experiments are conducted on server clusters with NVIDIA Tesla V100 GPUs. The summarize of the environments is gathered in Table 1. For Atari games, we need to point that IL with visual observations only is already very difficult [6]. However, learning policies for RAM-based observations is even more challenging [3, 27]. As far as we know, there are few IL researches reporting desirable results on this task. In our experiment, we investigate whether our algorithm can learn a good policy in Atari games with RAM-based observations from visual demonstrations under the HOIL setting.

Contenders. Four contenders are included in the experiments, which are variants of GAIL by including DSIL strategies: vallina GAIL [13] (**GAIL**), GAIL with importance-weighting (**GAIL-IW**), GAIL with third-person IL [26] (**GAIL-TP**), and GAIL with GAMA [18] (**GAIL-GAMA**). For GAIL-IW, we utilize the discriminator D_{w_1} in the previous stage to calculate the importance weight, also the optimization objective for the discriminator D_{w_2} in the current stage is the same as Equation (8); GAIL-TP learns the third-person demonstrations by leading the cross-entropy loss into the update of the feature extractor; GAMA learns a mapping function ϕ in view of adversarial training to align the observation of the target domain into the source domain, and thereby can utilize the policy in the source domain for zero-shot imitation. For fairness, we allow the interaction between the policy and the environment for GAIL-GAMA

Table 1: Environmental summary of the tasks.

Environment	Observation Space \mathcal{O}_E	Observation Space \mathcal{O}_L	Expert Rewards
Qbert	$84 \times 84 \times 4(\text{image})$	128(unsigned int)	4750.00 ± 50.51
ChopperCommand			3135.00 ± 145.86
Kangaroo			4175.00 ± 94.21
Hopper	8	9	522.84 ± 79.45
Humanoid	4	4	52.24 ± 1.29
Reacher	5	6	-8.99 ± 0.54
Swimmer	5	6	709.96 ± 75.54
Walker2d	188	188	536.58 ± 22.50

under HOIL. For Atari tasks, to investigate whether our method can achieve significant performance for RAM-based control, we further include a contender **PPO-RAM**, which uses PPO [24] to do reinforcement learning (RL) directly with the environmental rewards under the RAM-based observations.

Detailed setups. Considering query strategies, for GAIL-TP and GAIL-GAMA, if the output of the domain invariant discriminator is larger than 0.5, which means the encoder fails to generate proper features to confuse its discriminator, then we would store this data to update the encoder. For IWRE, the threshold of the rejection model g and the discriminator D_{w_2} is also 0.5, which means that if $g_2(\bar{x}) > 0.5$ meanwhile $D_{w_2}(\bar{x}) > 0.5$, the \mathcal{O}_E observation of this data would be queried. D_{w_2} , π_2 , and the encoder for GAIL-TP/GAIL-GAMA are pretrained for 100 epochs for all methods using evolving data before the current stage. The basic RL algorithm is PPO [24], and the reward signals of all methods are scaled into $[0, 1]$ to enhance the performance of RL. The buffer size for GAIL-TP and IWRE is set as 5000. Each time the buffer is full, the encoder and the rejection model will be updated for 4 epochs. We set all hyper-parameters, update frequency, and network architectures of the policy part the same to [9] (MIT License). Besides, the hyper-parameters of the discriminator for all methods are the same: rejection model and discriminator update using Adam with a decayed learning rate of $3e-4$; the batch size is 256. The ratio of update frequency between the learner and discriminator is 3: 1. The target coverage c in Equation (10) is set as 0.8. λ in Equation (10) is 1.0. All methods are implemented with Tensorflow [1] (Apache License).

Learning process. At the previous stage, we directly use GAIL/HashReward to train a policy π_1 and its reward function D_{w_1} in the \mathcal{O}_E space for MuJoCo/Atari environments. The learning steps are $1e7$ for MuJoCo and $5e6$ for Atari environments. At the evolving stage, we sample 20 trajectories from π_1 , and the data from each trajectory have both \mathcal{O}_E and \mathcal{O}_L observations. At the current stage, each method learns $4e7$ steps for MuJoCo and $2e7$ steps for Atari in the \mathcal{O}_L space to obtain π_2 .

5.2. Results

Experimental results in Atari and MuJoCo are reported in Figure 4. Since the mapping function is hard to learn when input RAM and output raw images, we omit the results of GAIL-GAMA in Atari. We can observe that while GAIL-IW is better than GAIL in most environments, both GAIL and GAIL-IW can hardly outperform π_1 . This is because that they just imitate the performance of π_1 instead of π_E , even though with importance-weighting to calibrate the learning process. For GAIL-TP, its learning process is extremely unstable on *Hopper*, *Swimmer* and *Walker2d* due to the continuous distribution shift in IL process. Furthermore, the performance of GAIL-GAMA is not satisfactory in *Hopper* and *Walker2d* because its mapping function is hard to be learned well when the support mismatch appears. Finally, as expected, IWRE obtains the best performance on all environments, which shows the effectiveness

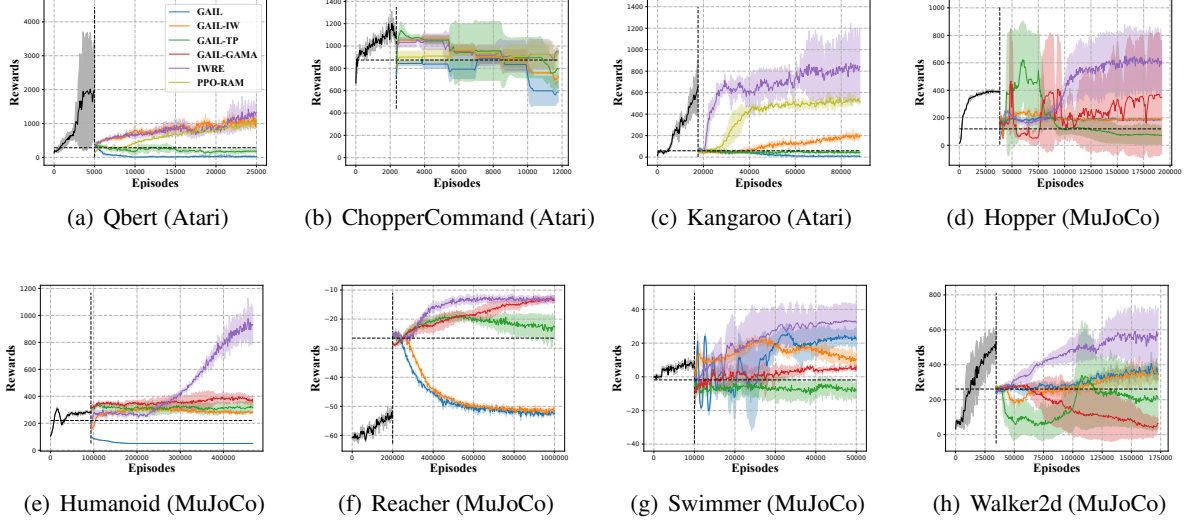


Figure 4: The learning curves of each method in Atari and MuJoCo environments, where shaded region indicates the standard deviation. The black curve denotes the performance of π_1 in \mathcal{O}_E space. The black vertical dotted line represents the dividing line between the previous and current stages, while the horizontal dotted line denotes the performance of behavior cloning.

of our method. Besides, we can see that the performance differences between the GAIL/GAIL-IW and IWRE/GAIL-TP/GAIL-GAMA are huge because of the absence of queries, which demonstrates that the query operation is indeed necessary for HOIL problems.

Moreover, we can observe that even learned with true rewards, PPO-RAM surprisingly fails to achieve comparable performance to IWRE, which shows that IWRE could possibly learn more meaningful rewards than true environmental rewards. The results prove that, with rejection and importance-weighting, IWRE provides a powerful approach for tackling HOIL problems, even the demonstrations are gathered from such a different observation space.

Distribution similarity on expert observations. As discussed in Section 4.2, the most challenging part of HOIL lies in dealing with the support mismatch due to $\text{supp}(\rho_{\pi_E}) \not\subseteq \text{supp}(\rho_{\pi_1})$. To find out whether IWRE has successfully carried out the latent part of demonstrations in the \mathcal{O}_E space by learning a policy in the \mathcal{O}_L space, we estimate distribution similarity by calculating the Wasserstein distance between the distribution of the expert demonstrations and each comparison methods. Since the original Wasserstein distance on multi-dimensional distributions is intractable, we provide the metric results and visualizations on two randomly selected dimensions of the \mathcal{O}_E space (20 trajectories for each method) in Figure 5. We can observe that the distance between IWRE and the expert is the smallest, even when compared with π_1 (i.e., data in the evolving stage). Besides, $\text{supp}(\pi_2.\text{IWRE})$ ideally cover $\text{supp}(\pi_E)$, which demonstrates that the superiority of IWRE indeed comes from successfully tackling the support mismatch problem.

6. Conclusion

In this paper, we proposed a new learning framework named *Heterogeneous Observations Imitation Learning* (HOIL), to formulate the situations where the observation space of demonstrations is different from that of the imitator while learning. We modeled the HOIL into a three-stage learning process, and

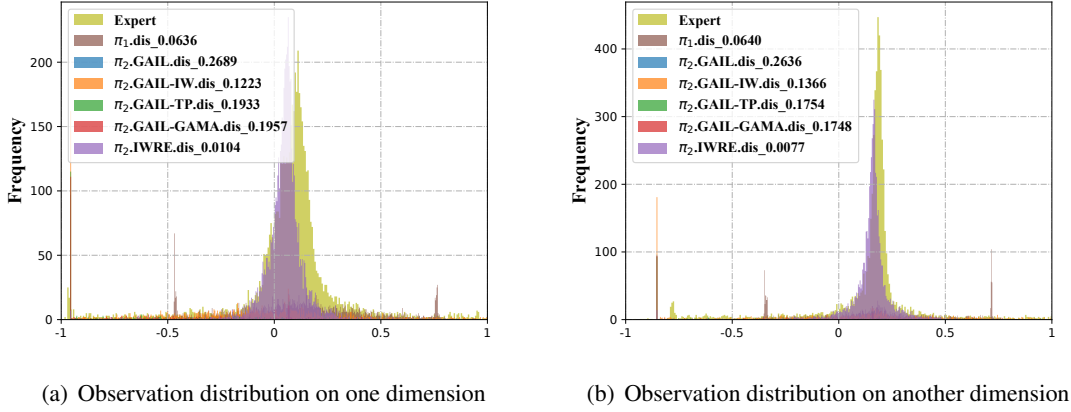


Figure 5: The visualizations of observation distribution on one dimension of \mathcal{O}_E space on *Walker2d*. “Expert” and “ π_1 ” make decision on \mathcal{O}_E space, while the rest methods make decision on \mathcal{O}_L space. “dis” denotes the Wasserstein distance between the distribution of the method and the demonstration.

further analyzed the most difficult part, i.e., the current stage, in which both the dynamics mismatch and the support mismatch on the occupancy distributions between the demonstrations and the policy will occur. To tackle these challenges, we proposed a new algorithm named IWRE using importance-weighting and learning with rejection. Experimental results showed that the direct imitation and domain adaptive methods cannot solve this problem, while our method can obtain promising results.

In real-world applications, there may not exist exact three stages as in HOIL. But currently we have validated the necessity of the three stages for HOIL in view of methodology and empirical studies. Lacking any of these stages without introducing new proper prior knowledge will lead to the failure of policy learning. Therefore, in the future, we hope to involve the theoretical guarantee for HOIL and investigate what property of the prior that satisfies can be used as an alternative to any of these three stages, and further use this learning framework and our algorithm IWRE to tackle more learning scenarios with demonstrations in different spaces.

Acknowledgment: This research was supported by NSFC (61921006) and KAKENHI (17H00757).

References

- [1] Martín Abadi, Ashish Agarwal, Paul Barham, Eugene Brevdo, Zhifeng Chen, Craig Citro, Greg S. Corrado, Andy Davis, Jeffrey Dean, Matthieu Devin, Sanjay Ghemawat, Ian Goodfellow, Andrew Harp, Geoffrey Irving, Michael Isard, Yangqing Jia, Rafal Jozefowicz, Lukasz Kaiser, Manjunath Kudlur, Josh Levenberg, Dandelion Mané, Rajat Monga, Sherry Moore, Derek Murray, Chris Olah, Mike Schuster, Jonathon Shlens, Benoit Steiner, Ilya Sutskever, Kunal Talwar, Paul Tucker, Vincent Vanhoucke, Vijay Vasudevan, Fernanda Viégas, Oriol Vinyals, Pete Warden, Martin Wattenberg, Martin Wicke, Yuan Yu, and Xiaoqiang Zheng. TensorFlow: Large-scale machine learning on heterogeneous systems, 2015. URL <https://www.tensorflow.org/>. Software available from tensorflow.org.
- [2] Christopher Amato and Frans A. Oliehoek. Scalable planning and learning for multiagent pomdps. In *Proceedings of the Twenty-Ninth AAAI Conference on Artificial Intelligence, January 25-30, 2015, Austin, Texas, USA*, pages 1995–2002, 2015.

- [3] Marc G. Bellemare, Yavar Naddaf, Joel Veness, and Michael Bowling. The arcade learning environment: An evaluation platform for general agents. *J. Artif. Intell. Res.*, 47:253–279, 2013.
- [4] Shai Ben-David, John Blitzer, Koby Crammer, Alex Kulesza, Fernando Pereira, and Jennifer Wortman Vaughan. A theory of learning from different domains. *Machine learning*, 79(1-2):151–175, 2010.
- [5] Greg Brockman, Vicki Cheung, Ludwig Pettersson, Jonas Schneider, John Schulman, Jie Tang, and Wojciech Zaremba. Openai gym. *CoRR*, abs/1606.01540, 2016.
- [6] Xin-Qiang Cai, Yao-Xiang Ding, Yuan Jiang, and Zhi-Hua Zhou. Imitation learning from pixel-level demonstrations by hashreward. In *Proceedings of the 20th International Conference on Autonomous Agents and Multi-Agent Systems (AAMAS)*, page 279–287, 2021.
- [7] Corinna Cortes, Giulia DeSalvo, and Mehryar Mohri. Learning with rejection. In Ronald Ortner, Hans Ulrich Simon, and Sandra Zilles, editors, *Algorithmic Learning Theory - 27th International Conference, ALT 2016, Bari, Italy, October 19-21, 2016, Proceedings*, volume 9925 of *Lecture Notes in Computer Science*, pages 67–82, 2016.
- [8] Siddharth Desai, Ishan Durugkar, Haresh Karnan, Garrett Warnell, Josiah Hanna, and Peter Stone. An imitation from observation approach to transfer learning with dynamics mismatch. In Hugo Larochelle, Marc’Aurelio Ranzato, Raia Hadsell, Maria-Florina Balcan, and Hsuan-Tien Lin, editors, *Advances in Neural Information Processing Systems 33: Annual Conference on Neural Information Processing Systems 2020, NeurIPS 2020, December 6-12, 2020, virtual*, 2020.
- [9] Prafulla Dhariwal, Christopher Hesse, Oleg Klimov, Alex Nichol, Matthias Plappert, Alec Radford, John Schulman, Szymon Sidor, Yuhuai Wu, and Peter Zhokhov. Openai baselines, 2017.
- [10] Tongtong Fang, Nan Lu, Gang Niu, and Masashi Sugiyama. Rethinking importance weighting for deep learning under distribution shift. In Hugo Larochelle, Marc’Aurelio Ranzato, Raia Hadsell, Maria-Florina Balcan, and Hsuan-Tien Lin, editors, *Advances in Neural Information Processing Systems 33: Annual Conference on Neural Information Processing Systems 2020, NeurIPS 2020, December 6-12, 2020, virtual*, 2020.
- [11] Yaroslav Ganin, Evgeniya Ustinova, Hana Ajakan, Pascal Germain, Hugo Larochelle, François Laviolette, Mario Marchand, and Victor Lempitsky. Domain-adversarial training of neural networks. *The Journal of Machine Learning Research*, 17(1):2096–2030, 2016.
- [12] Yonatan Geifman and Ran El-Yaniv. Selectivenet: A deep neural network with an integrated reject option. In Kamalika Chaudhuri and Ruslan Salakhutdinov, editors, *Proceedings of the 36th International Conference on Machine Learning, ICML 2019, 9-15 June 2019, Long Beach, California, USA*, volume 97 of *Proceedings of Machine Learning Research*, pages 2151–2159. PMLR, 2019.
- [13] Jonathan Ho and Stefano Ermon. Generative adversarial imitation learning. In *Advances in Neural Information Processing Systems 29: Annual Conference on Neural Information Processing Systems 2016, December 5-10, 2016, Barcelona, Spain*, pages 4565–4573, 2016.
- [14] Bo-Jian Hou, Lijun Zhang, and Zhi-Hua Zhou. Learning with feature evolvable streams. In Isabelle Guyon, Ulrike von Luxburg, Samy Bengio, Hanna M. Wallach, Rob Fergus, S. V. N. Vishwanathan, and Roman Garnett, editors, *Advances in Neural Information Processing Systems 30: Annual Conference on Neural Information Processing Systems 2017, December 4-9, 2017, Long Beach, CA, USA*, pages 1417–1427, 2017.

- [15] Chenping Hou and Zhi-Hua Zhou. One-pass learning with incremental and decremental features. *IEEE Trans. Pattern Anal. Mach. Intell.*, 40(11):2776–2792, 2018.
- [16] Shengyi Jiang, Jing-Cheng Pang, and Yang Yu. Offline imitation learning with a misspecified simulator. In *Advances in Neural Information Processing Systems 33: Annual Conference on Neural Information Processing Systems 2020, NeurIPS 2020, December 6-12, 2020, virtual*, 2020.
- [17] Kun Ho Kim, Yihong Gu, Jiaming Song, Shengjia Zhao, and Stefano Ermon. Cross domain imitation learning. *CoRR*, abs/1910.00105, 2019.
- [18] Kuno Kim, Yihong Gu, Jiaming Song, Shengjia Zhao, and Stefano Ermon. Domain adaptive imitation learning. In *Proceedings of the 37th International Conference on Machine Learning, ICML 2020, 13-18 July 2020, Virtual Event*, pages 5286–5295, 2020.
- [19] Bangalore Ravi Kiran, Ibrahim Sobh, Victor Talpaert, Patrick Mannion, Ahmad A. Al Sallab, Senthil Kumar Yogamani, and Patrick Pérez. Deep reinforcement learning for autonomous driving: A survey. *CoRR*, abs/2002.00444, 2020.
- [20] Shao-Yuan Li, Yuan Jiang, and Zhi-Hua Zhou. Partial multi-view clustering. In Carla E. Brodley and Peter Stone, editors, *Proceedings of the Twenty-Eighth AAAI Conference on Artificial Intelligence, July 27 -31, 2014, Québec City, Québec, Canada*, pages 1968–1974. AAAI Press, 2014.
- [21] Timothy P. Lillicrap, Jonathan J. Hunt, Alexander Pritzel, Nicolas Heess, Tom Erez, Yuval Tassa, David Silver, and Daan Wierstra. Continuous control with deep reinforcement learning. In Yoshua Bengio and Yann LeCun, editors, *4th International Conference on Learning Representations, ICLR 2016, San Juan, Puerto Rico, May 2-4, 2016, Conference Track Proceedings*, 2016.
- [22] Yuxuan Liu, Abhishek Gupta, Pieter Abbeel, and Sergey Levine. Imitation from observation: Learning to imitate behaviors from raw video via context translation. In *2018 IEEE International Conference on Robotics and Automation, ICRA 2018, Brisbane, Australia, May 21-25, 2018*, pages 1118–1125, 2018.
- [23] Shayegan Omidshafiei, Jason Pazis, Christopher Amato, Jonathan P. How, and John Vian. Deep decentralized multi-task multi-agent reinforcement learning under partial observability. In *Proceedings of the 34th International Conference on Machine Learning, ICML 2017, Sydney, NSW, Australia, 6-11 August 2017*, pages 2681–2690, 2017.
- [24] John Schulman, Filip Wolski, Prafulla Dhariwal, Alec Radford, and Oleg Klimov. Proximal policy optimization algorithms. *CoRR*, abs/1707.06347, 2017.
- [25] Pierre Sermanet, Corey Lynch, Yevgen Chebotar, Jasmine Hsu, Eric Jang, Stefan Schaal, and Sergey Levine. Time-contrastive networks: Self-supervised learning from video. In *2018 IEEE International Conference on Robotics and Automation, ICRA 2018, Brisbane, Australia, May 21-25, 2018*, pages 1134–1141, 2018.
- [26] Bradly C. Stadie, Pieter Abbeel, and Ilya Sutskever. Third person imitation learning. In *5th International Conference on Learning Representations, ICLR 2017, Toulon, France, April 24-26, 2017, Conference Track Proceedings*. OpenReview.net, 2017.
- [27] Jakub Sygnowski and Henryk Michalewski. Learning from the memory of atari 2600. In Tristan Cazenave, Mark H. M. Winands, Stefan Edelkamp, Stephan Schiffel, Michael Thielscher, and Julian

Togelius, editors, *Computer Games - 5th Workshop on Computer Games, CGW 2016, and 5th Workshop on General Intelligence in Game-Playing Agents, GIGA 2016, Held in Conjunction with the 25th International Conference on Artificial Intelligence, IJCAI 2016, New York City, NY, USA, July 9-10, 2016, Revised Selected Papers*, volume 705 of *Communications in Computer and Information Science*, pages 71–85.

- [28] Andrea Tirinzoni, Andrea Sessa, Matteo Pirotta, and Marcello Restelli. Importance weighted transfer of samples in reinforcement learning. In Jennifer G. Dy and Andreas Krause, editors, *Proceedings of the 35th International Conference on Machine Learning, ICML 2018, Stockholmsmässan, Stockholm, Sweden, July 10-15, 2018*, volume 80 of *Proceedings of Machine Learning Research*, pages 4943–4952. PMLR, 2018.
- [29] Emanuel Todorov, Tom Erez, and Yuval Tassa. Mujoco: A physics engine for model-based control. In *2012 IEEE/RSJ International Conference on Intelligent Robots and Systems, IROS 2012, Vilamoura, Algarve, Portugal, October 7-12, 2012*, pages 5026–5033.
- [30] Ruohan Wang, Carlo Ciliberto, Pierluigi Vito Amadori, and Yiannis Demiris. Random expert distillation: Imitation learning via expert policy support estimation. In Kamalika Chaudhuri and Ruslan Salakhutdinov, editors, *Proceedings of the 36th International Conference on Machine Learning, ICML 2019, 9-15 June 2019, Long Beach, California, USA*, volume 97 of *Proceedings of Machine Learning Research*, pages 6536–6544. PMLR, 2019.
- [31] Chang Xu, Dacheng Tao, and Chao Xu. A survey on multi-view learning. *CoRR*, abs/1304.5634, 2013.
- [32] Kaiqing Zhang, Zhuoran Yang, and Tamer Basar. Multi-agent reinforcement learning: A selective overview of theories and algorithms. *CoRR*, abs/1911.10635, 2019.
- [33] Zhenyu Zhang, Peng Zhao, Yuan Jiang, and Zhi-Hua Zhou. Learning with feature and distribution evolvable streams. In *Proceedings of the 37th International Conference on Machine Learning, ICML 2020, 13-18 July 2020, Virtual Event*, volume 119 of *Proceedings of Machine Learning Research*, pages 11317–11327. PMLR, 2020.

Algorithm 1 IWRE. π_1_Train

Input: Initialized policy π_1^0 ; Initialized reward function $D_{w_1}^0$; expert demonstration $\tilde{\mathcal{T}}_{\pi_E}$; Horizon in the previous stage T_1 .

Output: Policy under \mathcal{O}_1 space $\pi_1^{T_1}$; Reward function under \mathcal{O}_1 space $D_{w_1}^{T_1}$.

```
1: function  $\pi_1\_TRAIN(\pi_1^0, D_{w_1}^0, \tilde{\mathcal{T}}_{\pi_E}, T_1)$ 
2:   for  $t = 1, 2, \dots, T$  do
3:     Utilize  $\pi_1^{t-1}$  to sample  $\tilde{\mathcal{T}}_{\pi_1} \sim \rho_{\pi_1}$ .
4:     Sample a mini-batch  $\bar{x}_{\pi_1}$  and  $\tilde{x}_{\pi_E}$  from  $\tilde{\mathcal{T}}_{\pi_1}$  and  $\tilde{\mathcal{T}}_{\pi_E}$ .
5:     Update  $\pi_1^{t-1} \rightarrow \pi_2^t$  and  $D_{w_1}^{t-1} \rightarrow D_{w_1}^t$  by GAIL/HashReward with  $\bar{x}_{\pi_1}$  and  $\tilde{x}_{\pi_E}$ .
6:   end for
7:   return  $\pi_1^{T_1}, D_{w_1}^{T_1}$ 
8: end function
```

Algorithm 2 IWRE. π_1_Sample

Input: Policy trained in the previous stage $\pi_1^{T_1}$; Reward function trained in the previous stage $D_{w_1}^{T_1}$.

Output: Evolving data $\bar{\mathcal{T}}_{\pi_1}$; Reward function trained in the previous stage $D_{w_1}^{T_1}$; Rejection model g_1 and g_2^0 ; Pretrained policy for the current stage π_2^0 .

```
1: function  $\pi_1\_SAMPLE(\pi_1^{T_1}, D_{w_1}^{T_1})$ 
2:   Sample the evolving data  $\{\tilde{\mathcal{T}}_{\pi_1}, \bar{\mathcal{T}}_{\pi_1}\}$  by using  $\pi_1^{T_1}$ .
3:   Train  $g_1$  by Equation (10).
4:   Align  $g_1$  into  $g_2^0$  with  $\tilde{\mathcal{T}}_{\pi_1}$  and  $\bar{\mathcal{T}}_{\pi_1}$ .
5:   Train  $D_{w_1}^{T_1}$  with  $\tilde{\mathcal{T}}_{\pi_1}$ .
6:   Initialize  $\pi_2^0$  by behavior cloning with  $\bar{\mathcal{T}}_{\pi_1}$ .
7:   return  $\bar{\mathcal{T}}_{\pi_1}, D_{w_1}^{T_1}, g_1, g_2^0, \pi_2^0$ 
8: end function
```

A. Algorithm

The learning procedure of our algorithm is illustrated in Algorithms 1, 2, and 3.

B. Query Efficiency

We also investigate whether our query strategy is efficient. To this end, we allocate the query budget, i.e., limiting the query ratio for each method. For GAIL-TP, it preferentially queries those data with low D_{w_ϕ} output; for our method, it preferentially queries those data with high $\langle D_{w_2}, g_2 \rangle$ output. Besides, since GAIL and GAIL-IW cannot directly perform queries, we design a random-selection strategy for them as GAIL-Rand and GAIL-IW-Rand: for each batch of data, we randomly select data and input the \mathcal{O}_E observations of these data to D_{w_1} . If $D_{w_1}(x) > 0.5$, which means D_{w_1} regard this data being belonging to the expert demonstrations, then we would label this data as the expert data to update D_{w_2} . The results are depicted in Figure 6.

We can observe that the random strategy does not always improve the performance of GAIL and GAIL-IW. For GAIL-Rand, without importance-weighting to calibrate the learning process of the reward function, its performance become even worse on *Hopper*, *Swimmer*, and *Walker2d*, because the queried information

Algorithm 3 IWRE. π_2_Train

Input: Expert demonstrations $\tilde{\mathcal{T}}_{\pi_E}$; Reward function in the previous stage $D_{w_1}^{T_1}$; Rejection model g_1 and g_2^0 ; Evolving data $\bar{\mathcal{T}}_{\pi_1}$; Initialized policy and reward function π_2^0 and $D_{w_2}^0$; Buffer $\mathcal{B} = \emptyset$ in size of m_B ; Horizon in the current stage T_2 .

Output: Policy in the current stage $\pi_2^{T_2}$.

```
1: function  $\pi_2\_TRAIN(\tilde{\mathcal{T}}_{\pi_E}, D_{w_1}^{T_1}, g_1, g_2^0, \pi_2^0, D_{w_2}^0, \mathcal{B}, T_2)$ 
2:   for  $t = 1, 2, \dots, T_2$  do
3:     Sample  $\bar{\mathcal{T}}_{\pi_2} \sim \rho_{\pi_2}$  by using  $\pi_2^{t-1}$ .
4:     Sample a mini-batch  $\{\bar{x}_{\pi_2}\}$  and  $\{\bar{x}_{\pi_1}\}$  from  $\bar{\mathcal{T}}_{\pi_2}$  and  $\bar{\mathcal{T}}_{\pi_1}$ .
5:     Update  $\pi_2^{t-1} \rightarrow \pi_2^t$  by RL algorithms.
6:     Update  $D_{w_2}^{t-1} \rightarrow D_{w_2}^t$  by Equation (8) with  $\{\bar{x}_{\pi_2}\}$  and  $\{\bar{x}_{\pi_1}\}$ .
7:     if  $g_2(\bar{x}_{\pi_2}) = 1$  then
8:       Query the  $\mathcal{O}_1$  observation of  $\bar{x}_{\pi_2}$ , i.e.,  $\tilde{x}_{\pi_2}$ .
9:        $\mathcal{B} \leftarrow \mathcal{B} \cup \{\bar{x}_{\pi_2}, g_1(\tilde{x}_{\pi_2})\}$ .
10:      if  $|\mathcal{B}| = m_B$  then
11:        Update  $g_2^{t-1} \rightarrow g_2^t$  by Equation (10) with data in  $\mathcal{B}$ .
12:        Update  $D_{w_2}^t$  by Equation (8) with data in  $\mathcal{B}$ .
13:        Initialize  $\mathcal{B} \leftarrow \emptyset$ .
14:      end if
15:    end if
16:  end for
17:  return  $\pi_2^{T_2}$ 
18: end function
```

enhances the discrimination ability of reward function, making it even more impossible for the agent to obtain effective feedbacks; for GAIL-IW-Rand, its performance is better than GAIL-Rand on most environments, and is reinforced on *Hopper*, *Reacher*, and *Walker2d*, which further demonstrate that the query operation is indeed necessary for HOIL problem, but still fails compared with our method; for GAIL-TP, it is comparable with GAIL-IW-Rand, however, its performance improvement is very limited as the budget increases, and on *Swimmer* and *Walker2d* there even exist performance degradations, which suggests that its query strategy is very unstable; for GAIL-GAMA, it has a good start point, but the performance gain is very limited while the budget increases; for our method, its performance is almost the same as that of GAIL-IW-Rand without query on most environments. When it is allowed to query \mathcal{O}_E observation, our method outperforms other methods with a large gap, which shows that the query strategy of our method is indeed more efficient.

C. Imitation with Different # Expert Trajectories

The performances of different numbers of expert trajectories of all contenders are reported in Figure 7. We can observe that even with a very limited number of trajectories, our algorithm achieves better performance than other algorithms in most environments.

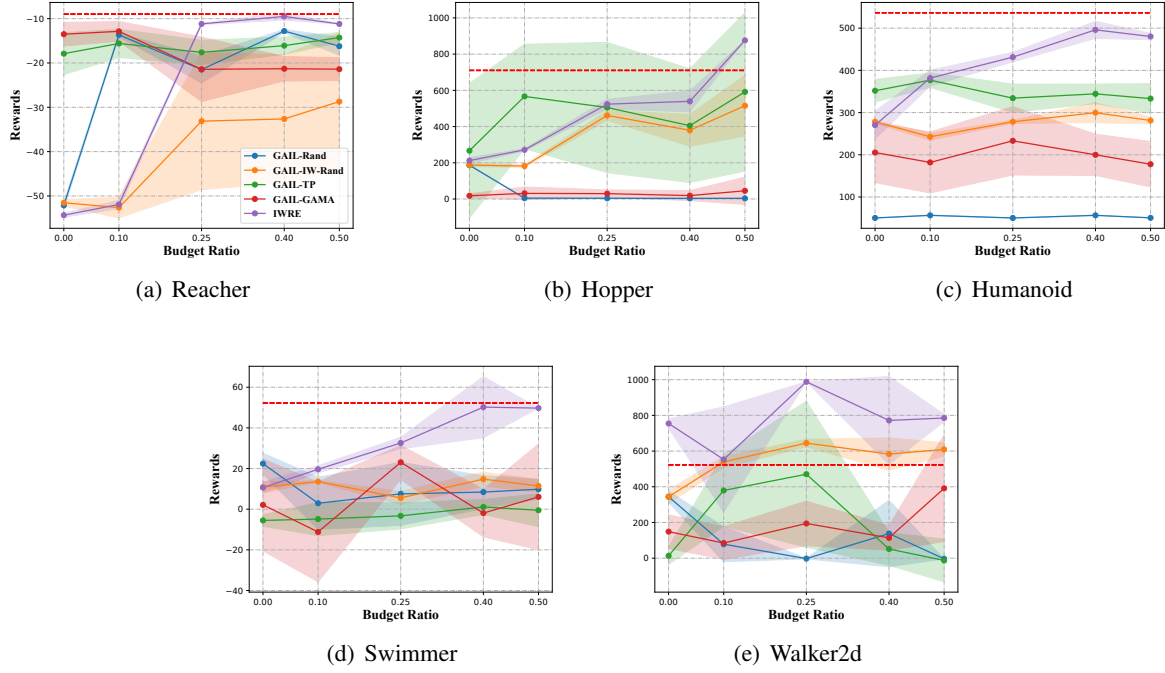


Figure 6: The final rewards of each method on MuJoCo with different budget ratios, where shaded regions indicate the standard deviation. The red horizontal dotted line represents the averaged performance of the expert.

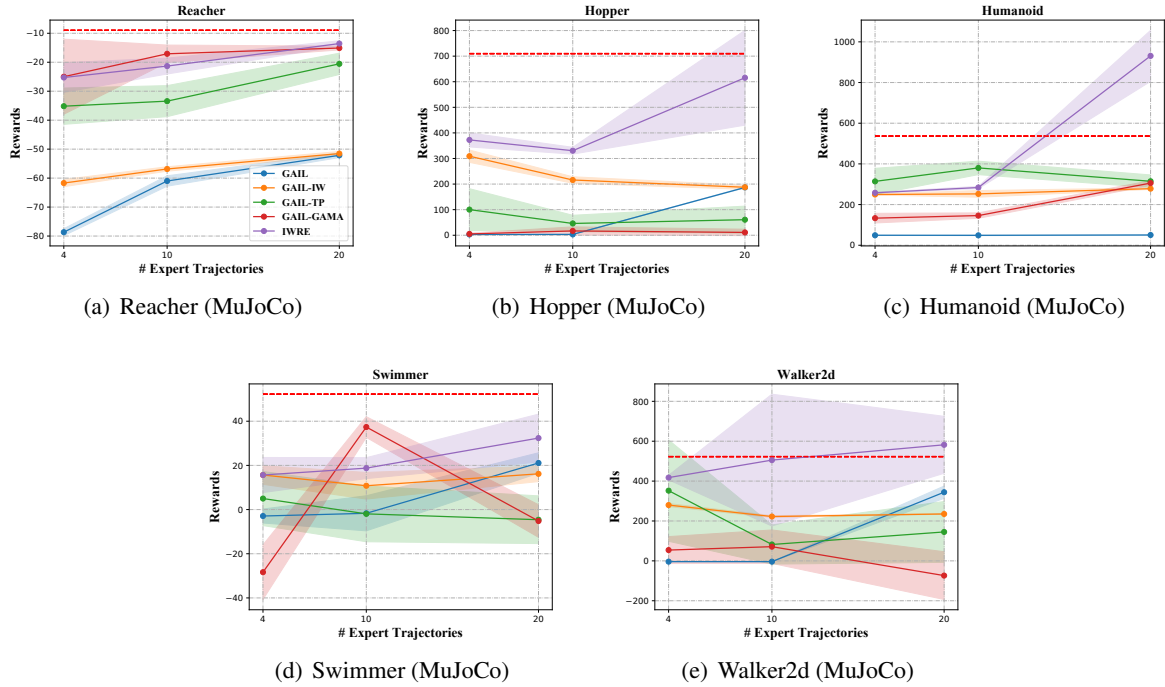


Figure 7: The learning curves of each method in MuJoCo environments with different number of expert trajectories, where shaded region indicates the standard deviations.